

Deep learning-based retinal abnormality detection from OCT images with limited data

Mohammad Talebzadeh ¹, Abolfazl Sodagartoji ², Zahra Moslemi ³, Sara Sedighi ⁴, Behzad Kazemi ^{5,*} and Faezeh Akbari ⁶

¹ Department of Civil and Environmental Engineering, Texas A&M University, USA.

² Department of Statistics, Rutgers University, USA.

³ Statistics Department, University of California, Irvine, USA.

⁴ Department of Electrical and Computer Engineering, Boise State University, Boise, ID, USA.

⁵ Department of Advanced Data Analytics, Toulouse Graduate School, University of North Texas, Denton, TX, USA

⁶ Department of Biomedical Engineering, University of Kentucky, Lexington, Kentucky, USA.

World Journal of Advanced Research and Reviews, 2024, 21(03), 690–698

Publication history: Received on 22 January 2024; revised on 29 February 2024; accepted on 02 March 2024

Article DOI: <https://doi.org/10.30574/wjarr.2024.21.3.0716>

Abstract

In the realm of medical diagnosis, the challenge posed by retinal diseases is considerable, given their potential to complicate vision and overall ocular health. A promising avenue for achieving highly accurate classifiers in detecting retinal diseases involves the application of deep learning models. However, overfitting issues often undermine the performance of these models due to the scarcity of image samples in retinal disease datasets. To address this challenge, a novel deep triplet network is proposed as a metric learning approach for detecting retinal diseases using Optical Coherence Tomography (OCT) images. Incorporating a conditional loss function tailored to the constraints of limited data samples, this deep triplet network enhances the model's accuracy. Drawing inspiration from pre-trained models such as VGG16, the foundational architecture of our model is established. Experiments use open-access datasets comprising retinal OCT images to validate our proposed approach. The performance of the suggested model is demonstrated to surpass that of state-of-the-art models in terms of accuracy. This substantiates the effectiveness of the deep triplet network in addressing overfitting issues associated with limited data samples in retinal disease datasets.

Keywords: Deep Triplet Network; Retinal Abnormalities; OCT; Deep Learning

1. Introduction

Formidable challenges confronting global ocular health emanate from conditions such as drusen, choroidal neovascularization (CNV), and diabetic macular edema (DME). The irreversible vision impairment prevalent among the elderly is chiefly ascribed to age-related macular degeneration (AMD), characterized by minute yellow deposits beneath the retina identified as drusen. CNV, linked to neovascular AMD, entails the aberrant proliferation of blood vessels beneath the retinal layers. AMD manifests a substantial annual incidence rate in the United States. The accumulation of fluid in the macula of adults with diabetes mellitus causes vision impairment due to DME, a common complication of diabetic retinopathy. Diabetic retinopathy can be treated with laser photocoagulation, intravitreal VEGF inhibitors, and corticosteroid injections to reduce inflammation and edema [42]. To prevent abnormal blood vessel growth and leakage in AMD, intravitreal anti-VEGF medications are administered [37]. Furthermore, certain situations may call for laser photocoagulation and photodynamic therapy (PDT). By implementing these interventions, the disease progression is decelerated, visual acuity is preserved, and further vision loss is prevented [1-2, 21-23, 25,29,33].

* Corresponding author: Behzad Kazemi

Retinal optical coherence tomography (OCT) is a crucial imaging technique used to capture detailed cross-sectional images of the retina while the patient is alive. It plays a vital role in diagnosing conditions like drusen, CNV, and DME by providing detailed and high-resolution retinal images. OCT is particularly useful in carefully analyzing the characteristics of drusen, detecting changes associated with CNV, and measuring macular thickness as well as fluid buildup in cases of DME. Despite its advantages, OCT image interpretation introduces subjectivity and variability among different observers, underscoring the imperative for standardized diagnostic methodologies. Ophthalmologists encounter challenges in the time-consuming analysis of OCT images, given the multitude of images generated per patient. The integration of machine learning and deep learning algorithms holds substantial promise in enhancing diagnostic precision through the scrutiny of OCT images. Additionally, OCT imaging has shown great potential in early detection and monitoring of various types of ocular cancers, paving the way for improved treatment outcomes and patient care [16-20,28,30,36,41].

Trained to identify intricate patterns linked to ocular conditions like drusen morphology and CNV-related changes, these algorithms enhance precision and reliability in detection. By undergoing rigorous training, they effectively address the challenges arising from subjectivity and variability in the interpretation of OCT images. This transformative capability positions artificial intelligence [39], particularly machine learning and deep learning algorithms, as powerful tools for refining the diagnostic accuracy of OCT imaging [1-2]

Recently, there has been a noticeable surge in the utilization of deep learning models for the analysis of medical imaging. Deep neural networks, operating as end-to-end learning models, demonstrate the ability to automatically extract features from medical images [3-4,32, 38,40]. Notably, deep learning algorithms have been increasingly applied to the categorization of OCT images. Various convolutional neural networks, including Inception V3, have been adapted for the classification of OCT images into four distinct classes: CNV, DME, Drusen, and Normal (Figure 1)[5]. Ensemble learning methods, leveraging ResNet152, have also been employed for this purpose [6]. Additionally, a modified ResNet50, combined with ensemble learning techniques, has been utilized to classify OCT images within the same predefined categories [7]. To train OCT images in these classes, a combination of image normalization and the VGG16 network has been applied [8]. In specific applications, four separate binary classifiers based on ResNet101 have been trained to discriminate cystoid macular edema, macular hole, epiretinal membrane, and serous macular detachment from OCT images [9]. It is noteworthy that, in the training of these convolutional neural networks, pre-trained weights derived from the ImageNet dataset have commonly served as initial weights or feature extractors [24,26,31]. These weights, obtained through the extensive training of image datasets, offer a valuable starting point for OCT image classification tasks.

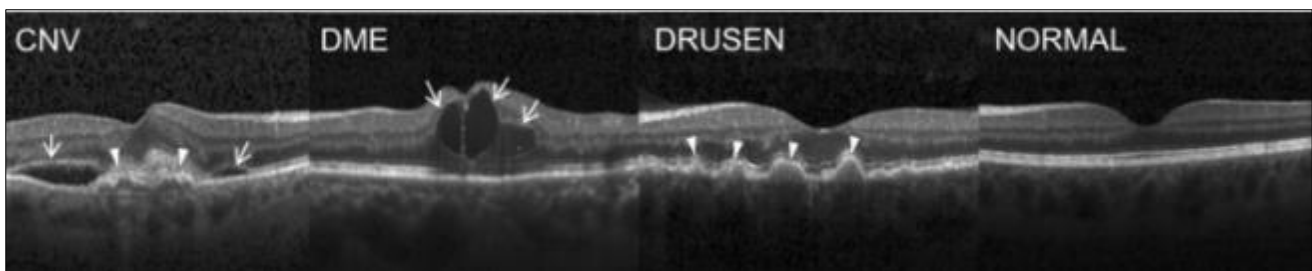


Figure 1 Representative Optical Coherence Tomography Images

In the realm of deep neural networks, a considerable amount of training data is typically demanded, presenting challenges when a wealth of examples is not readily available. In instances of limited data, the application of few-shot learning has been made use of to facilitate training with only a minimal number of examples. Through these algorithms, models can be effectively trained with just a few instances per class, enabling adaptation to unfamiliar categories without necessitating extensive retraining. Few-shot learning pursues two primary objectives: the establishment of robust generalization capabilities for new examples and the achievement of high accuracy, even when confronted with extremely limited data. Notably, metric learning has evolved into deep feature embedding networks utilizing measures such as Euclidean or cosine distance for comparisons between images. At the heart of the deep Triplet network lies a critical component: the loss term, which quantifies distinctions between images. The contrastive loss function, initially introduced to calculate the distance between two feature embeddings, aims to minimize the distance between pairs of images from the same class while simultaneously maximizing it between pairs from different classes. Subsequently, the Triplet loss function has emerged as one of the most widely adopted in deep Triplet networks. It is computed based on a triplet of samples—an anchor, a positive, and a negative data point—to reduce the distance between the anchor and the positive sample while increasing the distance between the anchor and the negative sample. The primary

contribution of this paper lies in the utilization of an enhanced Triplet deep neural network that incorporates a conditional loss, specifically employing the penalty-reward approach for the analysis of Optical Coherence Tomography (OCT) images. Our contributions in this paper encompass:

- A novel approach is introduced through the utilization of a deep Triplet network, where a new loss function is incorporated. The calculation of distances between the embedding features within the deep Triplet network is significantly influenced by this loss function. Through this enhancement, the network's capacity to discriminate and classify Optical Coherence Tomography (OCT) images is effectively elevated based on the relationships among their embedded features.
- A comprehensive experimental phase is undertaken in our study, wherein we apply our conditional Triplet network to a well-established public Optical Coherence Tomography (OCT) dataset. This dataset is widely recognized for its diverse compilation of retinal abnormalities, encompassing conditions like drusen, choroidal neovascularization (CNV), and diabetic macular edema (DME).

2. Material and methods

2.1. OCT Dataset

In this experimental study, we utilized an OCT dataset [10] sourced from publicly available data collected between 2013 and 2017 from five different institutes. The dataset comprises a total of 84,000 X-ray images, exhibiting a diversity of retinal conditions categorized into four distinct classes: the CNV class for choroidal neovascularization, the DME class for diabetic macular edema, the Drusen class highlighting the presence of drusen deposits, and the Normal class signifying cases where the retina exhibits normal characteristics. Although the dataset contains 84,000 images, we chose to work with a subset of this dataset for our model's training and evaluation in the case of limited data. This measured selection ensures a fair and consistent representation across all categories during both the training and evaluation phases.

2.2. Deep Triplet Network

In crafting our innovative neural network architecture, we introduce the Siamese deep neural network, a dual system comprising identical convolutional neural networks working in tandem [11, 27]. This unique design empowers the network to jointly process pairs of images, facilitating an intricate understanding of the interrelations between the features inherent in each image. These twin networks share identical structural designs, weights, and parameters, ensuring a synchronized learning process. The final layers of these networks produce distinctive feature embeddings for every input image. To evaluate the similarity between these feature embeddings, we employ the contrastive loss function. This function becomes the linchpin in our assessment mechanism. When the calculated distance between the feature embeddings falls below a predetermined threshold, it indicates that the two input images belong to the same class. Conversely, if the distance exceeds this threshold, it is a clear indicator that the two images belong to different classes. This innovative Siamese deep neural network architecture stands as a testament to our commitment to advancing the field of image processing and pattern recognition.

Building upon the Siamese network concept, the Deep Triplet network [12] introduces a novel approach by taking a triplet of samples as input, going beyond the traditional two-image setup. In the context of this study, the foundational architecture of our model is rooted in VGG16. The VGG16 [13] architecture consists of 13 convolutional layers, 5 max-pooling layers, and 3 fully connected layers, totaling 16 layers with adjustable parameters. This includes 13 convolutional layers and 3 fully connected layers. The initial block starts with 64 filters, and this count progressively doubles in subsequent blocks until reaching 512. It's important to note that our Triplet Network deviates from the VGG architecture by excluding the fully connected layers present in the original VGG16 design. Figure 2 illustrates the VGG16 architecture used in our study. This modification underscores our commitment to tailoring the network architecture for optimal performance in the context of triplet-based learning.

Shifting from the conventional deep Siamese network, a breakthrough has emerged with the Triplet network, where the Triplet loss has been identified as a key factor in elevating network performance. This pioneering approach introduces a triplet of input samples—consisting of an anchor, a positive, and a negative—which is then subjected to the Triplet loss. In this novel configuration, the anchor and positive samples share a common class, while the negative sample carries a distinct label. As these three samples traverse the network, their respective features are delineated in the final layer. Within the embedding space, the primary objective is to ensure proximity for images of the same class, resulting in well-defined and separate clusters [34,35]. The paramount goal is to facilitate the embedding of two examples with the same label in proximity within the embedding space, while concurrently maintaining a significant

distance between two examples with different labels. It is essential to underscore the precision required in the sample selection process, guaranteeing that the negative sample is positioned at a considerable distance from the positive sample by a predefined margin. This meticulous approach ensures the Triplet network's effective learning and discrimination capabilities, marking a paradigm shift in network architectures.

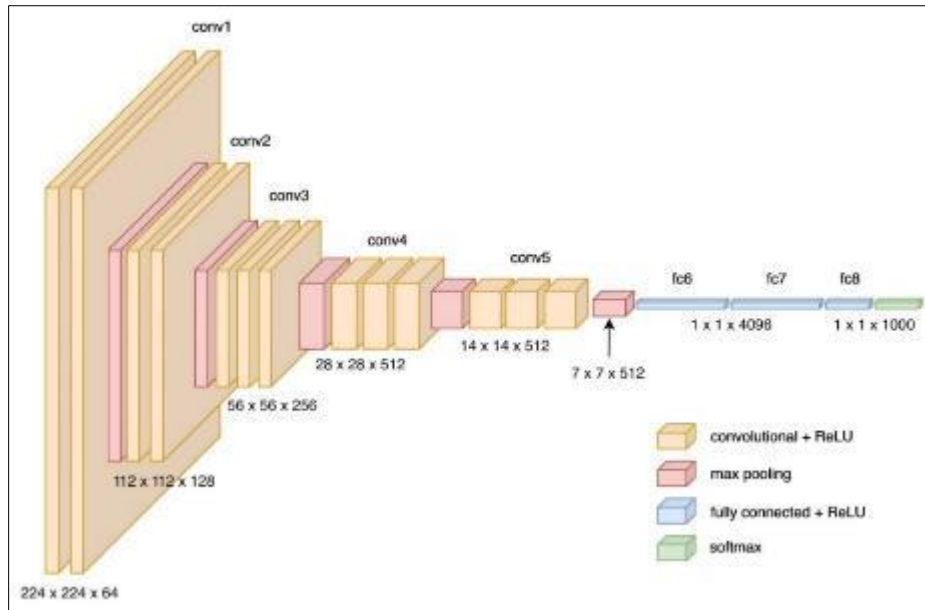


Figure 2 The Architecture of VGG16

2.3. Conditional Triplet Network

In the training phase of the deep Triplet network, a strategy of random sampling is employed for selecting triplet samples as inputs to the network. While random sampling proves computationally more efficient compared to more sophisticated methods, it does come with potential drawbacks such as slower convergence and the risk of being trapped in local optima. The standard Triplet loss faces a fundamental challenge in its uniform treatment of all triplets. To overcome this limitation, a conditional Triplet loss is implemented in our approach. This modified version introduces a penalty term for underperforming triplets and simultaneously provides rewards to triplets that satisfy the optimal condition (Figure 3) [14]. This adaptive strategy enhances the training process by offering more nuanced feedback to the network, fostering faster convergence and mitigating the risk of entrapment in local optima.

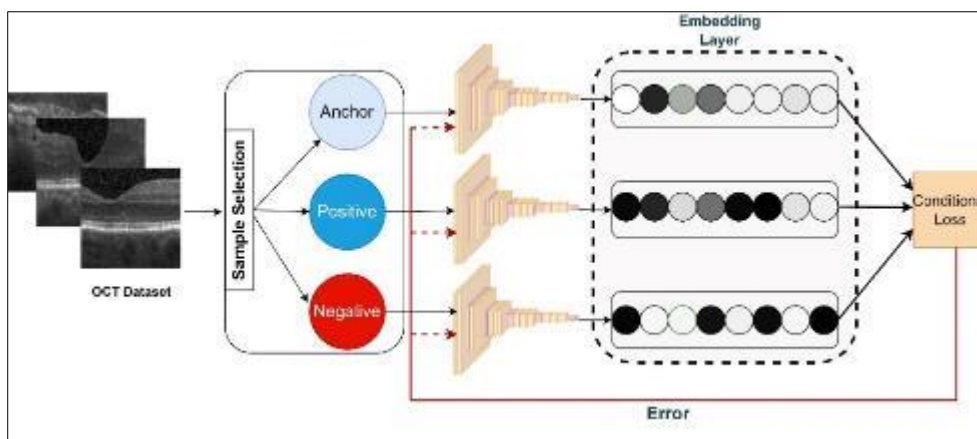


Figure 3 Our Selected Model

The significance of random sampling becomes apparent in the creation of diverse scenarios involving anchor, positive, and negative samples. Among these constructed triplets, the Triplet network prioritizes certain cases over others. Specifically, the network tends to favor samples that accelerate the convergence rate during training, while encountering difficulties with the worst triplets that hinder the network's training effectiveness. In situations identified

as the worst, the network's weights are updated inaccurately, leading to suboptimal training outcomes. To tackle this issue, our method involves identifying both the worst and best triplets. The worst-case occurs when the positive sample is positioned far from the anchor sample. Consequently, we introduce a penalty term to the Triplet loss function to mitigate the impact of these worst triplets, labeled as \mathcal{TW}_z in the loss function. Conversely, the best-case scenario arises when the distance falls within a specific small range, not significantly larger than zero, referred to as \mathcal{TB}_z [14]. In essence, the conditional loss function accommodates the standard Triplet loss for regular triplets, while worst and best triplets are handled differently as described above.

Varied samples combinations are generated through the process of random sampling within triplets. Within this set, two specific scenarios carry notable significance. Network convergence during training is expedited by the Triplet network's preference for samples that prove conducive to this process. Conversely, the worst triplets pose a challenge by potentially hindering training through incorrect weight updates. In cases deemed as the worst, where the positive sample significantly distances itself from the anchor, a resolution is implemented by introducing a penalty term to the Triplet loss, denoted as \mathcal{TW}_z . On the contrary, the best-case scenario manifests when the distance between samples falls within a specific small range, not significantly greater than zero, represented as \mathcal{TB}_z [14]. To summarize, the conditional loss distinguishes between the standard Triplet loss for regular triplets and the approach applied to the worst and best triplets, which are calculated as follows.:

$$loss(\mathcal{TW}_z) = \text{Max} [dis(x_a^z, x_p^z) - dis(x_a^z, x_n^z) + m, 0] + \alpha \times \left[\frac{dis(x_a^z, x_p^z) + dis(x_a^z, x_n^z)}{2} \right] \dots \dots \dots (1)$$

$$loss(\mathcal{TB}_z) = \text{Max} [dis(x_a^z, x_p^z) - dis(x_a^z, x_n^z) + m, 0] - \alpha \times \left[\frac{dis(x_a^z, x_p^z) - dis(x_a^z, x_n^z)}{2} \right] \dots \dots \dots (2)$$

As depicted in Figure 3, a triplet comprising an anchor, positive, and negative sample is simultaneously processed by three VGG16 networks, all possessing identical structural configurations. Each network produces embeddings for its corresponding samples. Subsequently, VGG16 undergoes training based on conditional loss.

3. Results and discussion

3.1. Parameter Setting

The implementation of the proposed conditional network in this study is carried out using Keras. All experiments are executed on an 8-core PC equipped with an i7-6900 processor operating at 3.8GHz and 16GB of RAM. A fixed margin of 0.2 is employed, random sampling is utilized, and the network undergoes training for 500 epochs. For experimentation, the OCT public dataset is employed, categorized into four classes: "Normal," "CNV," "DME," and "Drusen." Given the diverse sizes of images in the OCT dataset, normalization and image dimension scaling are performed to adapt the dataset to the required dimensions. In this research, 80% of these images are allocated for training and validation, while the remaining 20% are reserved for the testing dataset.

3.2. OCT Images Recognition

3.2.1. Experiments

As previously stipulated, the network facilitates the processing of three input images, each emblematic of distinct classes of retinal abnormalities, and orchestrates the generation of corresponding feature embeddings for each input. A pivotal step in this procedural paradigm involves the computation of the Euclidean distance between these generated feature embeddings. The overarching objective is to minimize this distance for paired images belonging to the same class and, conversely, maximize it for images originating from disparate classes. Consequently, the imposition of a predetermined threshold becomes imperative, affording the network the capacity to adjudicate class similarity: instances where the distance falls below the threshold imply a shared class designation.

In this investigative inquiry, the threshold is judiciously calibrated to uphold a False Positive Rate below 10e-3. Post the execution of the Siamese network employing the conditional triplet loss, sensitivity (recall) is scrutinized, quantifying the accurate identification of true positives. Sensitivity achieves its zenith at 89.4%. Subsequent juxtaposition of select test images with a reference image from each class reveals conspicuous patterns: the minimal Euclidean distance between test images and another image of the same class signifies close structural congruence. For instance, in the context of a test image affiliated with "CNV" (featured in the inaugural row of Figure 4), the Euclidean distance to an

intra-class sample approximates $1.8e-2$, while the distances to inter-class samples soar significantly, approximating $3.69e+1$ and $3.20e+1$.

3.2.2. Ablation Study

A simulation was conducted to assess the performance of the Triplet network proposed for recognizing Retinal OCT images. In this ablation study, we systematically examined the impact of each component on the network's overall performance. The simulation results unequivocally indicate that the proposed triplet loss method outperforms alternative approaches. Table 1 presents the modified Triplet loss excels beyond both the basic loss and the Siamese network in terms of sensitivity. Sensitivity (recall) is calculated as follows:

$$Recall = \frac{\text{Number of True Positives}}{\text{Number of True Positives} + \text{Number of False Negatives}} \dots \dots \dots (3)$$

3.3. Retinal Diseases Classification

The OCT dataset was utilized for the classification of Retinal diseases. The distribution of samples for each class is presented in Table 2. Instead of using all images, a portion of the dataset was employed. In this section, a predictive model for multi-class classification is implemented using an advanced deep Triplet network. Applying the proposed model to the selected OCT images yields an impressive overall accuracy of 92.81%.

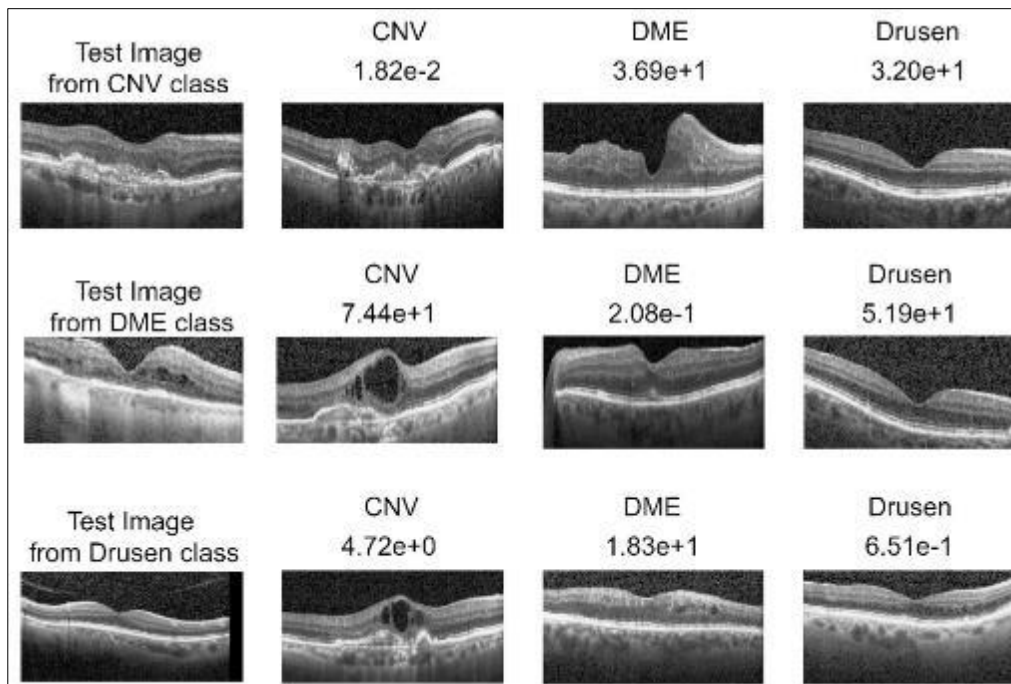


Figure 4 Some examples of the results

The performance of the proposed model is systematically contrasted with various established deep-learning models used in the classification of Retinal Diseases. These include DenseNet [15], InceptionV3 [5], Resnet152 [6], and ResNet50 [7], all of which have made substantial contributions to computer vision and image recognition. DenseNet, characterized by its densely connected convolutional networks, stands out for fostering dense connectivity, where each layer directly interacts with every other layer, facilitating feature reuse and efficient learning. InceptionV3, known for its inception modules, enables the network to capture features at multiple scales through parallel convolutional operations. Resnet152 and ResNet50, integral to the ResNet (Residual Network) family, introduced skip connections or residual blocks to mitigate the vanishing gradient problem, thereby enabling the training of significantly deeper networks. These models excel in both accuracy and depth. The experimental results demonstrate a clear superiority of the conditional triplet model over alternative approaches. Table 2 delineates the accuracy achieved by various models, with our proposed model notably outperforming others. It effectively addresses overfitting concerns, and enhances generalization, particularly on smaller datasets. It is crucial to note, however, that varying sample sizes may yield divergent outcomes. The accuracy of the model is computed as follows:

$$Accuracy = \frac{True\ Negatives + True\ Positives}{True\ Negatives + False\ Positives + False\ Negatives + True\ Positives} \dots \dots \dots (4)$$

Table 1 Results of an ablation study showing the recall (sensitivity) metric for the recognition task achieved by the selected model

Method	Recall (Sensitivity)
Siamese Net	72.28 ± 0.00010%
Triplet Net	78.62 ± 0.0035%
Triplet loss with penalty Net	87.66 ± 0.0030%
Triplet loss with penalty & reward Net	89.4 ± 0.0064%

Table 2 Comparison of model's accuracy with state-of-the-art techniques for Retinal diseases classification

Method	Model	Accuracy
Islam et al. [15]	DenseNet	92.64%
Kermany et al. [5]	InceptionV3	90.37%
Kim et al. [6]	Resnet152	91.86%
Li et al. [7]	ResNet50	91.48%
Our proposed	VGG16	92.81 %

4. Conclusion

This research addresses the challenge posed by limited data in the analysis of Retinal diseases using OCT images by implementing an advanced deep Triplet network. The model proposed incorporates a modified Triplet loss, accounting for both worst and best triplets. Subsequently, Retinal OCT images undergo classification into four classes for Retinal disease using the model. Drawing inspiration from VGG-16, the foundational architecture of our model is established. Simulation results are executed on a public OCT dataset, and a comparative analysis is conducted against existing state-of-the-art methods. The outcomes reveal the superior performance and accuracy of the proposed model, indicating its significant advantage over others in terms of accuracy.

Compliance with ethical standards

Disclosure of conflict of interest

No conflict of interest to be disclosed.

References

- [1] Sahl SJ, Hell SW, Fischer J, Otto T, Delori F, Pace L, Staurengi G, Aumann S, Donner S, Müller F, Müller PL. High resolution imaging in microscopy and ophthalmology. *Technology*. 2019 Aug 14;15.
- [2] Kim J, Tran L. Retinal disease classification from oct images using deep learning algorithms. In 2021 IEEE Conference on Computational Intelligence in Bioinformatics and Computational Biology (CIBCB) 2021 Oct 13 (pp. 1-6). IEEE.
- [3] Abbasi H, Orouskhani M, Asgari S, Zadeh SS. Automatic Brain Ischemic Stroke Segmentation with Deep Learning: A Review. *Neuroscience Informatics*. 2023 Sep 22:100145.
- [4] Shomal Zadeh F, Molani S, Orouskhani M, Rezaei M, Shafiei M, Abbasi H. Generative Adversarial Networks for Brain Images Synthesis: A Review. *arXiv e-prints*. 2023 May:arXiv-2305.

- [5] Kermany DS, Goldbaum M, Cai W, Valentim CC, Liang H, Baxter SL, McKeown A, Yang G, Wu X, Yan F, Dong J. Identifying medical diagnoses and treatable diseases by image-based deep learning. *cell*. 2018 Feb 22;172(5):1122-31.
- [6] Kim J, Tran L. Ensemble learning based on convolutional neural networks for the classification of retinal diseases from optical coherence tomography images. In 2020 IEEE 33rd International Symposium on Computer-Based Medical Systems (CBMS) 2020 Jul 28 (pp. 532-537). IEEE.
- [7] Li F, Chen H, Liu Z, Zhang XD, Jiang MS, Wu ZZ, Zhou KQ. Deep learning-based automated detection of retinal diseases using optical coherence tomography images. *Biomedical optics express*. 2019 Dec 1;10(12):6204-26.
- [8] Li F, Chen H, Liu Z, Zhang X, Wu Z. Fully automated detection of retinal disorders by image-based deep learning. *Graefe's Archive for Clinical and Experimental Ophthalmology*. 2019 Mar 4;257:495-505.
- [9] Lu W, Tong Y, Yu Y, Xing Y, Chen C, Shen Y. Deep learning-based automated classification of multi-categorical abnormalities from optical coherence tomography images. *Translational vision science & technology*. 2018 Nov 1;7(6):41-.
- [10] <https://www.kaggle.com/datasets/paultimothymooney/kermany2018>
- [11] Koch G, Zemel R, Salakhutdinov R. Siamese neural networks for one-shot image recognition. In *ICML deep learning workshop 2015* Jul 10 (Vol. 2, No. 1).
- [12] Hoffer E, Ailon N. Deep metric learning using triplet network. In *Similarity-Based Pattern Recognition: Third International Workshop, SIMBAD 2015, Copenhagen, Denmark, October 12-14, 2015. Proceedings 3 2015* (pp. 84-92). Springer International Publishing.
- [13] Simonyan K, Zisserman A. Very deep convolutional networks for large-scale image recognition. *arXiv preprint arXiv:1409.1556*. 2014 Sep 4.
- [14] Shi D, Orouskhani M, Orouskhani Y. A conditional Triplet loss for few-shot learning and its application to image co-segmentation. *Neural Networks*. 2021 May 1;137:54-62.
- [15] Islam KT, Wijewickrema S, O'Leary S. Identifying diabetic retinopathy from oct images using deep transfer learning with artificial neural networks. In 2019 IEEE 32nd international symposium on computer-based medical systems (CBMS) 2019 Jun 5 (pp. 281-286). IEEE.
- [16] Taher AS, Sadrabad MJ, Izadi A, Ghorbani R, Sohanian S, Saberian E. The Effect of Dentin Matrix Proteins on Differentiation of Autologous Guinea Pig Dental Pulp Stem Cells. *Journal of the Scientific Society*. 2023 May 1;50(2):214-9. DOI: 10.4103/jss.jss_186_22
- [17] Saberian E, Jenča A, Petrášová A, Jenčová J, Jahromi RA, Seiffadini R. Oral Cancer at a Glance. *Asian Pacific Journal of Cancer Biology*. 2023 Oct 22;8(4):379-86.
- [18] Sadrabad MJ, Ghahremanfard F, Sohanian S, Mobarhan M, Nabavi A, Saberian E. Knowledge and attitude of cancer patients' companions towards chemotherapy and radiotherapy-induced oral complications and dental considerations. *Iran Red Crescent Med J*. 2023 February; 25(2):e2133. <https://doi.org/10.32592/ircmj.2023.25.2.2133>
- [19] Sadrabad MJ, Pedram A, Saberian E, Emami R. Clinical efficacy of LLLT in treatment of trigeminal neuralgia—Case report. *Journal of Oral and Maxillofacial Surgery, Medicine, and Pathology*. 2023 Nov 1;35(6):568–71. <https://doi.org/10.1016/j.ajoms.2023.03.012>.
- [20] Sadrabad MJ, Saberian E. Plasma Therapy for Medication-Related Osteonecrosis of the Jaws—A Case Report. *Case Reports in Clinical Practice*. 2023 Jul 17;8(1):1-4. <https://doi.org/10.18502/crcp.v8i1.13088>.
- [21] Velisdeh ZJ, Najafpour GD, Mohammadi M, Poureini F. Optimization of Sequential Microwave-Ultrasound-Assisted Extraction for Maximum Recovery of Quercetin and Total Flavonoids from Red Onion (*Allium cepa* L.) Skin Wastes. *arXiv preprint arXiv:2104.06109*. 2021 Apr 13. <https://doi.org/10.48550/arXiv.2104.06109>
- [22] Maghsoudloo M, Bagheri Shahzadeh Aliakbari R, Jabbari Velisdeh Z. Pharmaceutical, nutritional, and cosmetic potentials of saponins and their derivatives. *Nano Micro Biosystems*. 2023 Dec 1;2(4):1-6. <https://doi.org/10.22034/NMBJ.2023.416018.1027>
- [23] Shineh G, Mobaraki M, Afzali E, Alakija F, Velisdeh ZJ, Mills DK. Antimicrobial Metal and Metal Oxide Nanoparticles in Bone Tissue Repair. *Biomedical Materials & Devices*. 2024 Feb 5:1-24. <https://doi.org/10.1007/s44174-024-00159-3>
- [24] Loghmani N, Moqadam R, Allahverdy A. Brain Tumor Segmentation using Multimodal MRI and Convolutional Neural Network. In 2022 30th International Conference on Electrical Engineering (ICEE) 2022 May 17 (pp. 227-230). IEEE. <https://doi.org/10.1109/ICEE55646.2022.9827274>

- [25] Ebadi M, Ebrahimimonfared M, Sadeghi R, Ashtiani AR, Mofrad AM, Faraji F, Mohammadi M. Migraine Symptoms In Patients With MRI White Matter Hyperintensity After And Before Treatment. *Journal of Positive School Psychology*. 2022 Jul 24;6(7):40-7.
- [26] Dehghani, F., & Larijani, A. (2023). Average portfolio optimization using multi-layer neural networks with risk consideration. Available at SSRN. <https://dx.doi.org/10.2139/ssrn.4436648>
- [27] Hashemi A, Jang J, Beheshti J. A Machine Learning-Based Surrogate Finite Element Model for Estimating Dynamic Response of Mechanical Systems. *IEEE Access*. 2023, 11, 54509-54525. <https://doi.org/10.1109/ACCESS.2023.3282453>
- [28] Gorgzadeh A, Hheidari A, Ghanbarikondori P, Arastonejad M, Goki TG, Aria M, Allahyartorkaman A, Moazzam F. Investigating the properties and cytotoxicity of cisplatin-loaded nano-polybutylcyanoacrylate on breast cancer cells. *Asian Pacific Journal of Cancer Biology*. 2023 Nov 6;8(4):345-50.
- [29] Sabzevari P, Abady FH, Araghian S, Bahramian F, Isanezhad A. The Effectiveness of Existential Therapy Intervention on Anxiety Caused by Coronavirus and Death. *Clinical Cancer Investigation Journal*. 2022;11(1s):1-7.
- [30] Lima B, Razmjouei S, Bajwa MT, Shahzad Z, Shoewu OA, Ijaz O, Mange P, Khanal S, Gebregiorgis T. Polypharmacy, gender disparities, and ethnic and racial predispositions in long QT syndrome: an in-depth review. *Cureus*. 2023 Sep 26;15(9), e46009. <https://doi.org/10.7759/cureus.46009>
- [31] Vahdatpour MS, Sajedi H, Ramezani F. Air pollution forecasting from sky images with shallow and deep classifiers. *Earth Science Informatics*. 2018 Sep;11:413-22. <https://doi.org/10.1007/s12145-018-0334-x>
- [32] Lai W, Kuang M, Wang X, Ghafariasl P, Sabzalian MH, Lee S. Skin cancer diagnosis (SCD) using Artificial Neural Network (ANN) and Improved Gray Wolf Optimization (IGWO). *Scientific Reports*. 2023 Nov 8;13(1):19377. <https://doi.org/10.1038/s41598-023-45039-w>
- [33] Jafari B, Gholizadeh E, Jafari B, Zhoulideh M, Adibnia E, Ghafariasl M, Noori M, Golmohammadi S. Highly sensitive label-free biosensor: graphene/CaF₂ multilayer for gas, cancer, virus, and diabetes detection with enhanced quality factor and figure of merit. *Scientific Reports*. 2023;13(1):16184.
- [34] Song C, Guo J, Gholizadeh F, Zhuang J. Quantitative Analysis of Food Safety Policy—Based on Text Mining Methods. *Foods*. 2022;11(21):3421. <https://doi.org/10.3390/foods11213421>
- [35] Dutta A, Masrourisaadat N, Doan TT. Convergence Rates of Decentralized Gradient Dynamics over Cluster Networks: Multiple-Time-Scale Lyapunov Approach. In *2022 IEEE 61st Conference on Decision and Control (CDC)*, 2022, (pp. 6497-6502). IEEE. <https://doi.org/10.1109/CDC51059.2022.9992900>
- [36] Schwarz G, Horestani FJ. Prediction of Breast Cancer Recurrence With Machine Learning. In *Encyclopedia of Information Science and Technology, Sixth Edition, 2025* (pp. 1-33). IGI Global. <https://doi.org/10.4018/978-1-6684-7366-5.ch061>
- [37] Pahnkolaei SM, Kachabi A, Sipey MH, Ganji DD. New approach method for solving nonlinear differential equations of blood flow with nanoparticle in presence of magnetic field. *arXiv preprint arXiv:2402.16208*. 2024. <https://doi.org/10.48550/arXiv.2402.16208>
- [38] Moslemi Z, Meng Y, Lan S, Shahbaba B. Scaling up bayesian neural networks with neural networks. *arXiv preprint arXiv:2312.11799*. 2023. <https://doi.org/10.48550/arXiv.2312.11799>
- [39] Farrokhi, M., Moeini, A., Taheri, F., Farrokhi, M., Mostafavi, M., Ardakan, A. K., ... & Faranoush, P. (2023). Artificial Intelligence in Cancer Care: From Diagnosis to Prevention and Beyond. *Kindle*, 3(1), 1-149.
- [40] Manshour N, He F, Wang D, Xu D. Integrating Protein Structure Prediction and Bayesian Optimization for Peptide Design. In *NeurIPS 2023 Generative AI and Biology (GenBio) Workshop 2023*. <https://openreview.net/forum?id=CsjGuWD7hk>
- [41] Aghamohammadghasem M, Azucena J, Hashemian F, Liao H, Zhang S, Nachtmann H. System simulation and machine learning-based maintenance optimization for an inland waterway transportation system. In *2023 Winter Simulation Conference (WSC) 2023 Dec 10* (pp. 267-278). IEEE. <https://doi.org/10.1109/WSC60868.2023.10408112>
- [42] Mirmiranpour H, Amjadi A, Khandani S, Shafae Y, Sobhani SO. Wavelength Effect in Laser Therapy of Diabetic Rats on Oxidants: AGEs, AOPP, ox-LDL Levels. 2020; 6(2): 17-24. <https://doi.org/10.11648/j.ijcems.20200602.11>